Chinese Journal of Oceanology and Limnology
Vol. 34 No. 4, P. 672-682, 2016
http://dx.doi.org/10.1007/s00343-016-5017-1

Size-fractionated Chlorophyll *a* biomass in the northern South China Sea in summer 2014*

LIU Haijiao (刘海娇)[1, 2], XUE Bing (薛冰)[1, 2], FENG Yuanyuan (冯媛媛)[1, 2], ZHANG Rui (张锐)[3], CHEN Mianrun (陈绵润)[4], SUN Jun (孙军)[1, 2, **]

[1] *College of Marine Science and Engineering, Tianjin University of Science and Technology, Tianjin 300457, China*

[2] *Tianjin Key Laboratory of Marine Resources and Chemistry, Tianjin University of Science and Technology, Tianjin 300457, China*

[3] *State Key Laboratory of Marine Environmental Science and the Institute of Marine Microbes and Ecospheres, Xiamen University, Xiamen 361102, China*

[4] *Institute of South China Sea Planning and Environment, State Oceanic Administration (SOA), Guangzhou 510300, China*

Received Jan. 21, 2015; accepted in principle Mar. 27, 2015; accepted for publication Apr. 14, 2015

Abstract Spatial distribution of phaeopigment and size-fractionated chlorophyll *a* (Chl *a*) concentrations were examined in relation to hydrographic conditions in the northern South China Sea (NSCS) during a survey from 20 August to 12 September, 2014. The total Chl *a* concentration varied from 0.006 to 1.488 μg/L with a mean value of 0.259±0.247 (mean±standard deviation) μg/L. Chl *a* concentration was generally higher in shallow water (<200 m) than in deep water (>200 m), with mean values of 0.364±0.311 μg/L and 0.206±0.192 μg/L respectively. Vertically, the maximum total Chl *a* concentration appeared at depths of 30–50 m and gradually decreased below 100 m. The size-fractionated Chl *a* concentrations of grid stations and time-series stations (SEATS and J4) were determined, with values of pico- (0.7–2 μm), nano- (2–20 μm) and micro- plankton (20–200 μm) ranging from 0.001–0.287 (0.093±0.071 μg/L), 0.004–1.149 (0.148±0.192 μg/L) and 0.001–0.208 (0.023±0.036 μg/L), respectively. Phaeopigment concentrations were determined at specific depths at ten stations, except for at station A9, and varied from 0.007 to 0.572 (0.127±0.164) μg/L. Nano-and pico-plankton were the major contributors to total phytoplankton biomass, accounting for 50.99%±15.01% and 39.30%±15.41%, respectively, whereas microplankton only accounted for 9.39%±8.66%. The results indicate that the contributions of microplankton to total Chl *a* biomass were less important than picoplankton or nanoplankton in the surveyed NSCS. Different sized-Chl *a* had similar spatial patterns, with peak values all observed in subsurface waters (30–50 m). The summer monsoon, Kuroshio waters, Zhujiang (Pearl) River plume, and hydrological conditions are speculated to be the factors controlling the abundance and spatial heterogeneity of Chl *a* biomass in the NSCS.

Keyword: Northern South China Sea; size-fractionated chlorophyll *a*; phaeopigment; picoplankton; Zhujiang (Pearl) River

1 INTRODUCTION

The South China Sea (SCS) is the largest semi-closed deep marginal sea, covering an area of 3 500 000 km^2. Due to monsoons, it is characterized by extreme seasonal variations (Su, 2005; Hu et al., 2014). There are complex biogeographic and hydrological features in the northern South China Sea (NSCS), affected by coastal eutrophic water and deep basin oligotrophic water (Gong et al., 1992).

Investigations on phytoplankton distribution in the SCS can be traced back to the 1970s. Guo et al. (1978) and Ye et al. (1983) led preliminary studies of netz-

* Supported by the Program for New Century Excellent Talents in University (No. NCET-12-1065), the Ocean Public Welfare Scientific Research Project (No. 201105021-03), the National Natural Science Foundation of China (Nos. 41276124, 41176136), the Science Fund for University Creative Research Groups in Tianjin (No. TD12-5003), the Key Project of National Natural Science Foundation of Tianjin (No. 12JCZDJC30100) to J Sun, and the National Natural Science Foundation of China (No. 41306118) to Y Feng
** Corresponding author: phytoplankton@163.com

phytoplankton, whereas Le et al. (2006) and Sun et al. (2007) reported phytoplankton community and spatial patterns. Peng et al. (2006) elucidated the dynamics of phytoplankton growth by nutrient enrichment. Furthermore, Chen et al. (2006) studied the features of phytoplankton communities in an upwelling region and warm eddy waters, respectively. More recently, Ma and Sun (2014) depicted the phytoplankton community and its controlling factors in the summer and winter. Phytoplankton assemblages of small-scale regional areas (Nansha Island, Daya Bay, Zhujiang (Pearl) River) have also been surveyed (Song et al., 2002; Li et al., 2005, 2008; Wang et al., 2006, 2009; Ho et al., 2010; Qiu et al., 2010; Shen et al., 2010).

The marine chlorophyll *a* (Chl *a*) content represents the standing stock of phytoplankton in a region (Le and Ning, 2006), with the Chl *a* abundance and pattern denoting the structure and density of the phytoplankton community (Zhou et al., 2004). Previous studies have reported the distribution of total Chl *a* (Ning et al., 2004; Zhao et al., 2005; Zhang et al., 2007; Le et al., 2008; Lin et al., 2010), and size-fractionated Chl *a* (Liu et al., 1998; Che et al., 2012) in the SCS. In oligotrophic oceans, small Chl *a* fractions are major contributors to phytoplankton biomass and the microbial food web (Berman et al., 1986; Azov, 1991; Polat and Aka, 2007). Indeed, up to 50% of total Chl *a* biomass was contributed by picoplankton in some regions (Gieskes et al., 1979; Platt et al., 1983; Odate and Maita, 1989; Iriarte and Purdie, 1994). However, large temporal-spatial heterogeneity has been observed in Chl *a* structure in the aforementioned studies. Diurnal fluctuations in Chl *a* concentration may have coincided with diurnal photosynthesis periodicity, and this relationship can be numerically estimated (Shimada, 1958; Yentsch and Ryther, 2003). Chl *a* consumed by zooplankton can be degraded into phaeopigments and non-fluorescent materials (Helling and Baars, 1985). Chl *a* degradation into phaeopigment is often caused by zooplankton grazing, bacterial activity, autolytic cell lysis and cell sinking. Phaeopigment was abundantly distributed in sediments (Bianchi et al., 1991; Fundel et al., 1998; Zhao et al., 2010). Wide variety of degradation products can be acted as indicators of grazing activity (Jeffrey, 1980). The sinking fecal materials also can be reingested by bathypelagic predators located at differed depths and was preserved in their guts (Lorenzen et al., 1983). Hence, proportions of phaeopigments can be used to interpret carbon transfer and transmission efficiency in the marine carbon cycle.

In this study, the spatial distribution and variation of size-fractionated Chl *a* and phaeopigment in the NSCS were examined. Special emphasis was placed on determining the heterogeneity of different sized Chl *a* and observing the Chl *a* dynamics at two mooring stations. Time-series studies at two stations were also conducted, to understand the diurnal variations in Chl *a* biomass. In addition, the relationship between the distribution of the size-fractionated Chl *a* concentration and dissolved inorganic nutrient concentrations was studied. The information presented fills our knowledge gap in understanding the spatial and temporal variations in size fractionated Chl *a* and phaeopigment concentrations, and their relationship with environmental controllers of biological characteristics in the NSCS.

2 MATERIAL AND METHOD

2.1 Sample collection and analysis

Field routine sampling was conducted during the summer cruise of the R/V *Shi Yan 1* in August/September 2014. The eleven sampling stations are shown in Fig.1 including two times-series stations (SEATS and J4). The bottom depths from the nearshore to offshore stations were 28 m, 46 m, 71 m, 76 m, 106 m, 141 m, 737 m, 2 176 m, 2 671 m, 3 754 m and 3 846 m respectively. At each station, water samples were taken for Chl *a* measurement at seven depths (5 m, 25 m, 50 m, 75 m, 100 m, 150 m, and 200 m) using Niskin bottles on a rosette sampler (SEA-BIRD SCIENTIFIC, Seabird SBE 17 plus). Vertical temperature and salinity profiles of the water column were obtained from the Seabird CTD profiler.

For nutrient analysis, seawater samples were filtered through 47-mm, 0.22-μm pore-size Millipore cellulose acetate membrane filters and refrigerated at -20°C prior to measurements. Dissolved inorganic nutrient concentrations, including NO_3-N, NO_2-N, SO_3-Si and PO_4-P, were examined using an Auto-Analyser3 (Bran + Luebbe) (SEAL, Germany), based on continuous flow injection analysis.

2.2 Pigment analysis and size fractionation

Chl *a* concentrations were determined onboard, using the fluorescence method followed by Parsons et al. (1984). Sub-samples (<200 m: 0.5–1 L; >200 m: 2–4 L) were filtered serially through 20 μm×20 mm silk net, 2 μm×20 mm nylon membrane, and

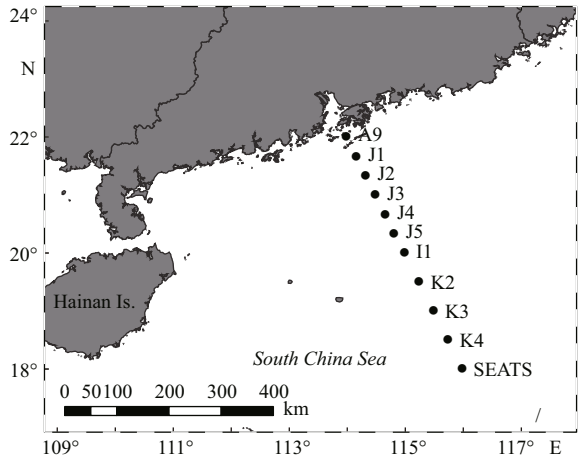

Fig.1 Sampling sites in the NSCS from 20 August–12 September 2014, with two time-series stations (SEATS & J4)

Circles represent sampling stations.

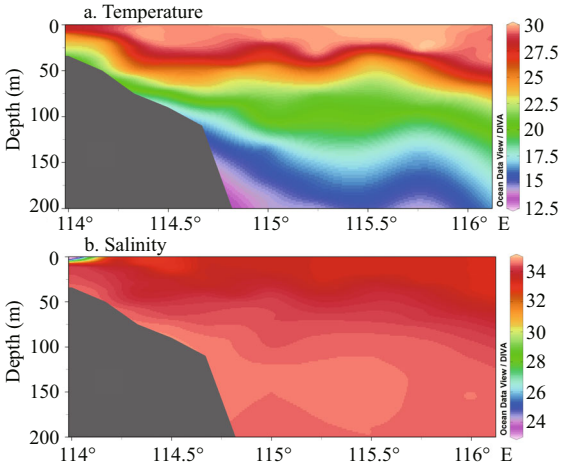

Fig.2 Transectional distribution of temperature and salinity in the euphotic zone (<200 m)

0.7 μm×47 mm Whatman GF/F filters for size-fractionated Chl *a* analysis under a filtration vacuum of less than 100 mm Hg. The filters were placed into 20-mL glass tubes, the pigments were then extracted by 5 mL 90% acetone, and stored in the dark at 4°C for 24 h. The Chl *a* contents was then measured using a CE Turner Designs Fluorometer.

Phaeopigment concentrations were obtained from 3–5 water depths at ten stations, with the exception of station A9. Phaeopigment was quantified using the same method as total Chl *a*. Following extraction in acetone 90%, the fluorescence of phaeopigment retained by Whatman GF/F filters was determined before and after acidification.

2.3 Statistical analysis

The depth-weighted Chl *a* concentration was calculated following the trapezoid integration formula:

$$P=\left\{\sum_{i=1}^{n-1}\frac{P_{i+1}+P_i}{2}(D_{i+1}-D_i)\right\}/D\,,$$

where P is the mean value of the water column Chl *a* concentration, P_i is the Chl *a* concentration at layer i, D is the maximum sampling depth, D_i is the depth at layer i, and n is the number of sampling layers. The calculation expressed above is referred to as the depth-weighted value, assuming homogeneity within the water column other than the depth-integrated value (column burden).

All contour maps were created using Surfer 10 program (Golden Software, Inc) and Ocean Data View 4.5 (ODV) software (Schlitzer, 2010). Color scatter diagrams and linear regressions were processed by OriginPro 8.5.0 software. Temporal and spatial fluctuations in depth and diel data, and size-fractionated Chl *a* were tested statistically using parametric or nonparametric tests on the analysis of variance (SPSS 19.0 software).

3 RESULT AND DISCUSSION

3.1 Environmental factors

Water column temperature and salinity, recorded from August to September 2014, varied from 14.25–29.95 (22.43±5.02)°C and 23.62–34.61 (34.15±0.66), respectively. The mean sea surface temperature and salinity were 29.49±0.55°C and 33.08±0.86, respectively. Vertical profiles of temperature suggested that the water column was well stratified throughout the entire sampling area. Vertically homogeneous high salinity occupied all stations, with the exception of station A9, where temperature was high and salinity was low (Fig.2). The water column at SEATS and adjacent regions had high temperature and high salinity (Figs.3, 4). The mean salinity of coastal (<200 m) and pelagic water (>200 m) was 33.77 and 34.24, respectively (Fig.4). At the two time-series stations of SEATS (Fig.5a and c) and J4 (Fig.5c and d), the vertical distribution of temperature and salinity in the seawater column was temporally stable.

3.2 Chl *a* concentration and distribution pattern

3.2.1 Total Chl *a* and phaeopigment

Total Chl *a* concentrations ranged from 0.006 to 1.488 μg/L, with an average of 0.259±0.247 μg/L. The lowest Chl *a* concentration was observed in the 200 m

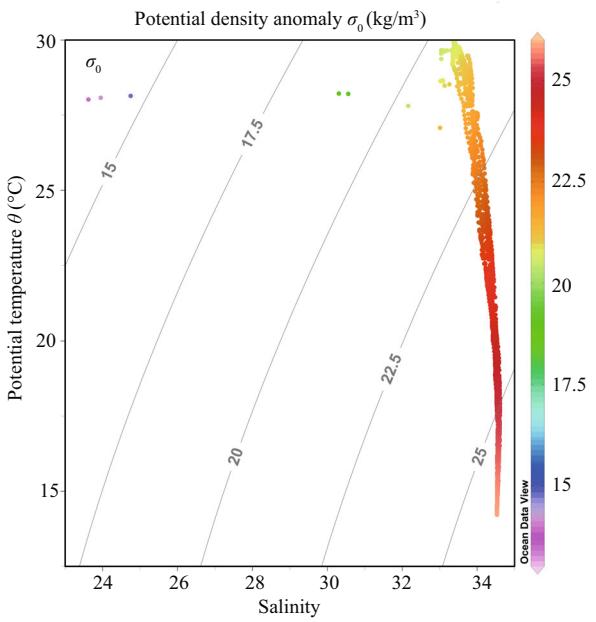

Fig.3 Temperature and salinity in the NSCS water layers shallower than 200 m

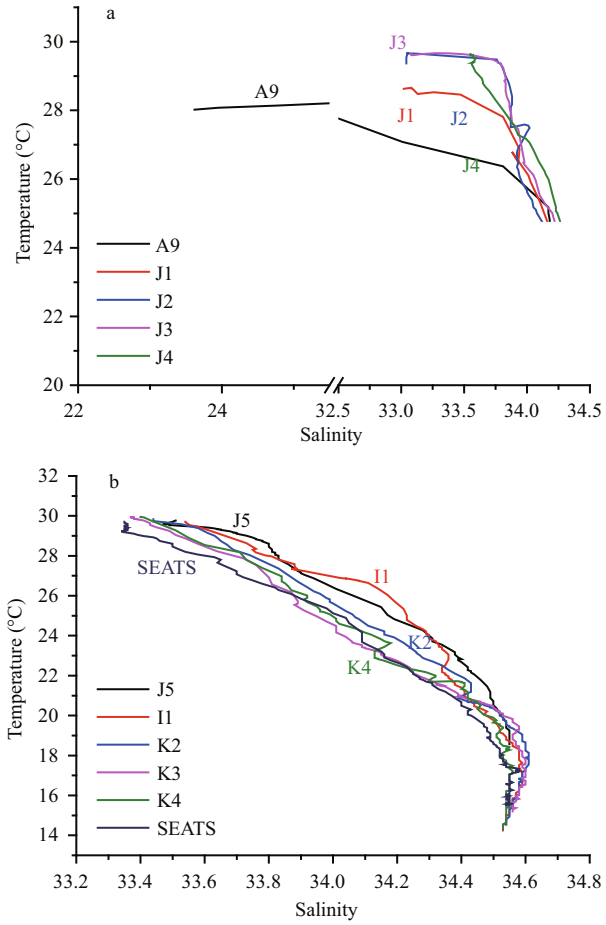

Fig.4 Coupled diagrams between temperature and salinity in coastal and pelagic regimes

a. depth shallower than 200 m; b. depth below 200 m.

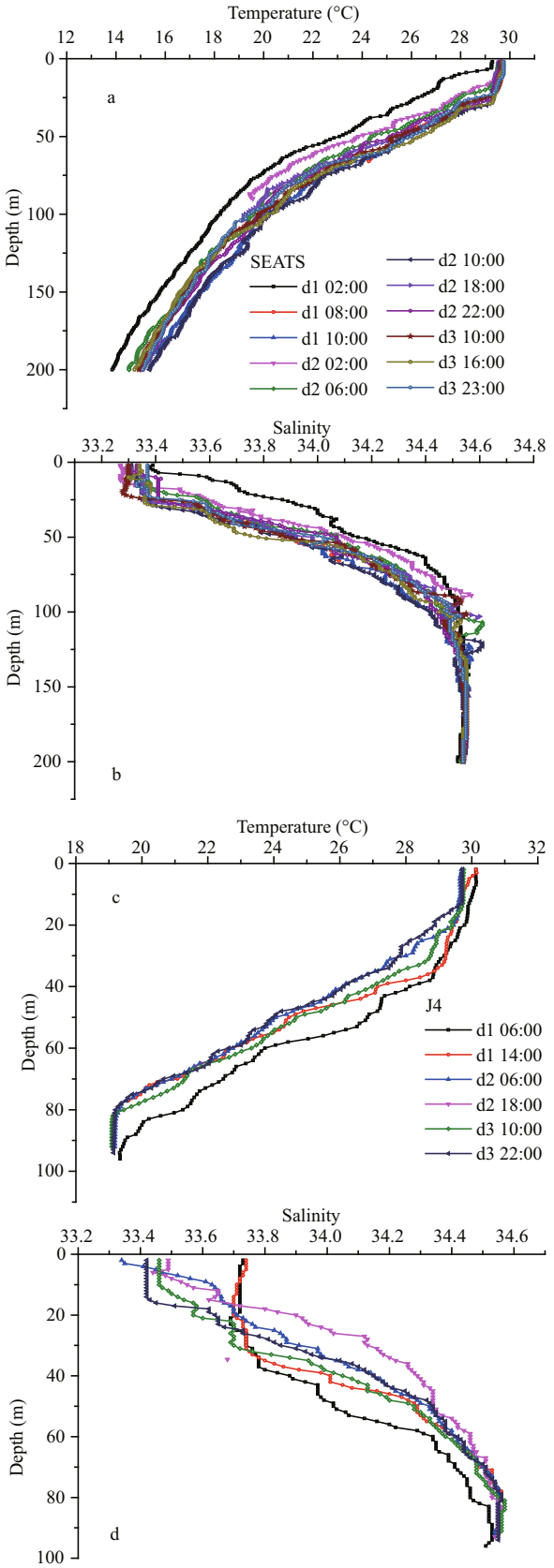

Fig.5 Vertical distributions of temperature and salinity at the two time-series stations

a, b. SEATS; c, d. J4.

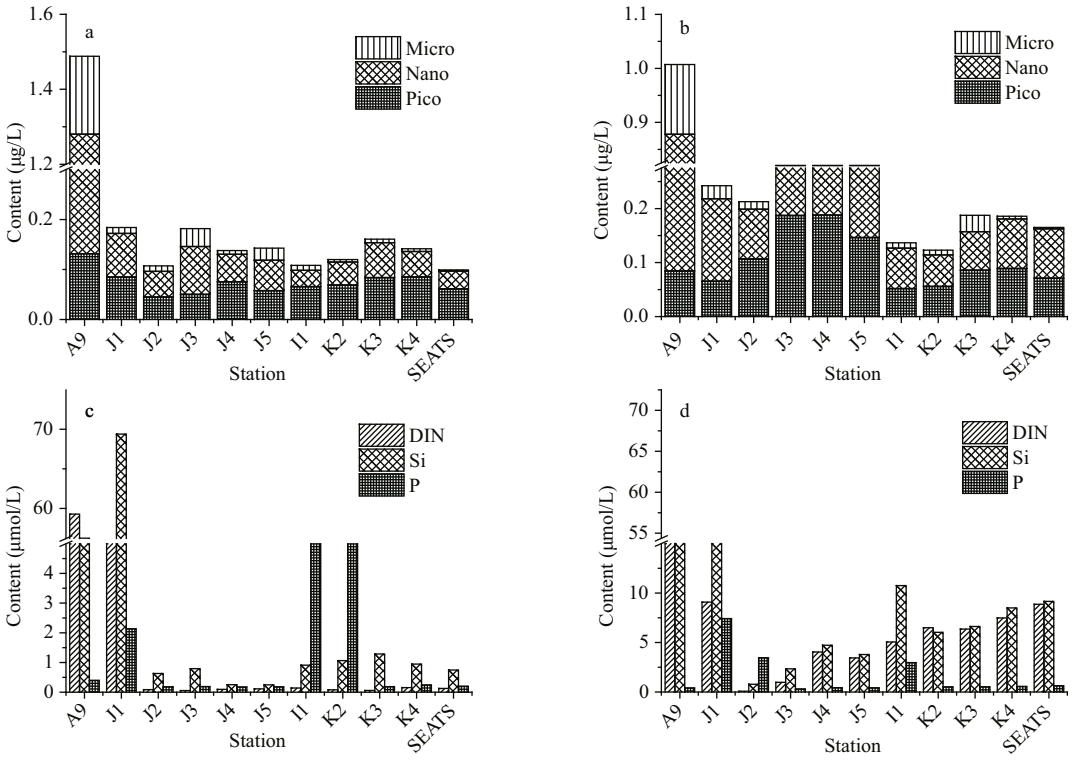

Fig.6 Size-fractionated Chl *a* contributions to total Chl *a* biomass and nutrient composition

a. Chl *a* in surface water; b. depth-weighted Chl *a* in the water column; c. nutrients in surface water; d. depth-weighted nutrients in the water column.

water layer at station K2 and the highest in the surface layer of station A9, which was closest to the Zhujiang River discharge (Fig.6a). The Chl *a* concentration in the coastal domain was much higher than in the offshore area. The depth-weighted Chl *a* concentration varied between 0.145 and 1.007 μg/L (0.321± 0.250 μg/L). The contributions of various Chl *a* fractions was shown in Fig.6a, b. It was observed that the percentage contribution of picoplankton was higher in deep basin waters than in shallow waters. During periods of low Chl *a* biomass, a higher proportion of the pico fraction was observed (Iriarte and Purdie, 1994). Chl *a* was generally higher in shallow water (<200 m) than in deep water (>200 m), with mean values of 0.364±0.311 μg/L and 0.206±0.192 μg/L, respectively. In our study, examining the size-fractioned Chl *a* indicated that the contribution of picoplankton to total Chl *a* biomass, both for the surface layer (Fig.6a) and the depth-weighted water column (Fig.6b), increased from the coastal area to the pelagic regions. This is probably caused by the variable nutrient concentrations in different regions: the macronutrient concentrations (such as nitrate and phosphate, see Fig.6c) were, in general, lower in the offshore areas compared to the coastal waters. Owing to their small size, picoplankton has an advantage over other phytoplankton groups in nutrient absorption dynamics in oligotrophic waters (Jiao and Ni, 1997); this would, therefore, explain the relatively higher average percentage of picoplankton Chl *a* in the deep-water basins (>200 m) than that of shallow (<200 m) waters (Fig.7). Except for at station A9, the total Chl *a* biomass peaked in the subsurface layer (30–50 m) (Fig.8a). In the present study, the Deep Chlorophyll Maximum (DCM) was located at 50–75 m in the SCS, with homogenous concentrations between 100–200 m (Fig.8).

Phaeopigment values (Fig.8e) ranged from 0.007 to 0.572 (0.127±0.164 μg/L) and the depth-weighted value was 0.111–0.453 (0.127±0.157 μg/L). Phaeopigment showed increasing from the offshore area to the nearshore area. Phytoplankton and zooplankton were highly abundant, due to eutrophication resulting from the Zhujiang River plume. Strong grazing activity induces numerous degradation products, typically phaeopigment (Suzuki and Fujita, 1986; Fundel et al., 1998).

3.2.2 Size-fractionated Chl *a*

The maximal Chl *a* concentrations of all size classes were observed in the inshore area, except for picoplankton (Fig.8). In addition, the nano- class

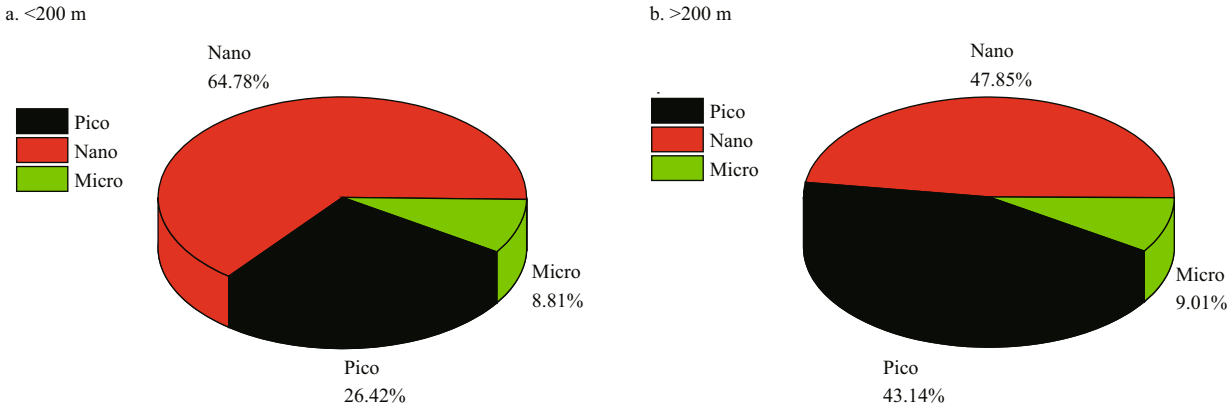

Fig.7 Size-fractionated Chl *a* contributions to total Chl *a* biomass (as percentages of depth-weighted data) in (a) shallow (<200 m) and (b) deep basin (>200 m) waters

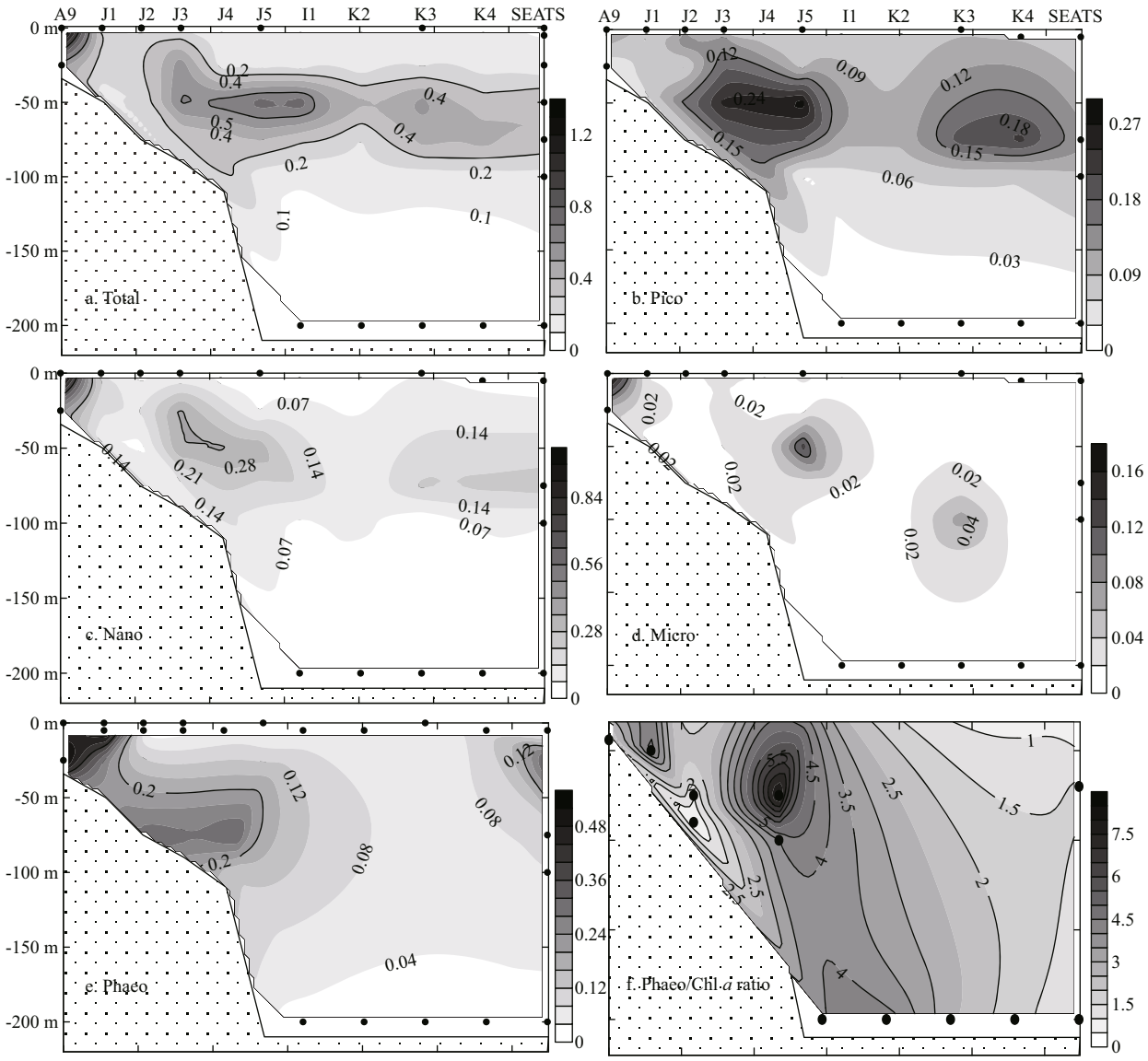

Fig.8 Vertical profiles of Chl *a* (μg/L), phaeopigment (μg/L) and the phaeopigment/Chl *a* ratio in the survey area

a. total Chl *a*; b. pico-size; c. nano-size; d. micro-size; e. phaeopigment; f. phaeopigment/Chl *a* ratio.

Table 1 Vertical distribution of average size-fractionated Chl *a* concentrations (n represents the number of samples)

Depth (m)	Micro (μg/L) (>20 μm)	Nano+pico (μg/L) (<20 μm)	Total (μg/L)	*n*
0	0.021±0.035	0.115±0.152	0.244±0.249	6
5	0.023±0.023	0.101±0.086	0.223±0.185	8
25	0.015±0.035	0.099±0.088	0.249±0.243	5
50	0.018±0.025	0.109±0.097	0.078±0.091	5
75	0.018±0.043	0.090±0.084	0.066±0.079	6
100	0.018±0.043	0.085±0.081	0.062±0.075	6
200	0.012±0.017	0.117±0.166	0.050±0.063	5

showed higher values at water depths of 25 m and 50 m at station J3 and 50 m at station J4 (0.365, 0.344, 0.363 μg/L), but lower than depth of 0 m at station A9 (1.149 μg/L) (Fig.8c). Relatively higher values of the pico- class were observed at station J3, J4 and J5, compared with those in the neighboring waters (Fig.8b). The highest concentration of pico- class Chl *a* (0.287 μg/L) was found at ~50 m water depth at station J5. Table 1 shows the value of size-fractionated Chl *a* at each sampling depth. A comparison among size fractions showed clearly that the <20-μm fraction (nano- plus pico-plankton) accounted for a larger proportion of overall Chl *a* than any other size class of Chl *a*, throughout the entire period of study.

There was a significant difference (Kruskal-Wallis test; $P<0.05$) in Chl *a* fractions among the three group depths (Table 2). The seven depth data was compiled into three groups based on vertical temperature pattern (Fig.2); the upper mixed layer (0–50 m), DCM (75 m) and bottom layer (100–200 m).

3.3 Chl *a* concentration at time-series stations

Two time-series stations were investigated to understand the diurnal fluctuations in phytoplankton biomass, by measuring the size-fractionated Chl *a* concentrations. Diurnal variation in phytoplankton Chl *a* biomass was observed at both stations, but were not significantly different (One-way ANOVA, $\alpha=0.05$).

3.3.1 Total Chl *a*

Time-series observations were conducted at 6-hour intervals over 3 days at station SEATS (Fig.9a–d), and at 12-hour intervals over 3 days at station J4 (Fig.9c–h). The average Chl *a* biomass at stations SEATS and J4 was 0.232±0.181 and 0.307±0.179 μg/L, respectively. At station SEATS, the total Chl *a* concentration was generally higher at 75 m, than in other water layers. At station J4, the maximum total Chl *a* concentration was observed at a water depth of 50 m. Irradiance, temperature, nutrient uptake and carbon assimilation were the factors most likely to be controlling the distribution of the Chl *a* maxima, based on previous studies (Shimada, 1958; Goering et al., 1964; Yentsch and Ryther, 2003). In Yentsch and Ryther (2003), a Chl *a* maxima occurred in the morning and afternoon, and decreased at midday and at night. In our study, there were two peaks, at water depths of 75 m at 14:00 and 12:00 at station SEATS, mainly composed of picoplankton biomass. Similarly, Ning et al. (2004) concluded that phytoplankton biomass was primarily comprised of picoplankton in the SCS area. One peak occurred at 50 m at station J4 at 14:00. In the present study, the total phytoplankton Chl *a* biomass reached a maximum during the daytime. This is consistent with the hypothesis that phytoplankton tends to propagate in the daytime to make good use of the sunlight, furthermore, the dynamics of Chl *a* biomass are probably affected by zooplankton grazing and diurnal vertical migration of phytoplankton (Tang and Chen, 2006).

Table 2 Kruskal-Wallis tests for depth effects on Chl *a* fractions (pico, nano and micro) (df, rank and significance level *P* are shown; $\alpha=0.05$)

Size fraction	df	χ^2	*P*
Pico	2	17.369	0.000
Nano	2	11.669	0.003
Micro	2	10.040	0.007

3.3.2 Size-fractionated Chl *a*

Temporal variations in the contribution of each fraction to the phytoplankton biomass is shown in Fig.9. The pico- size fraction at station SEATS peaked in the daytime at 08:00, 14:00 and 06:00 with a maximum value of 0.476 μg/L, and then decreased at dusk (Fig.9b). At station SEATS, variations in the nano-size fraction were similar to the pico-size fraction. In these waters, the micro-size has the smallest average contribution (5.95±7.32%). The phytoplankton biomass was dominated by the pico- and nano-fraction. Their proportions are larger in more oligotrophic waters (Polat and Aka, 2007). At station J4, the mean level of nano-size fraction Chl *a* concentration was highest across all size fractions. The highest concentrations of nano- (0.573 μg/L, Fig.9g) and micro- (0.072 μg/L, Fig.9h) size Chl *a* at

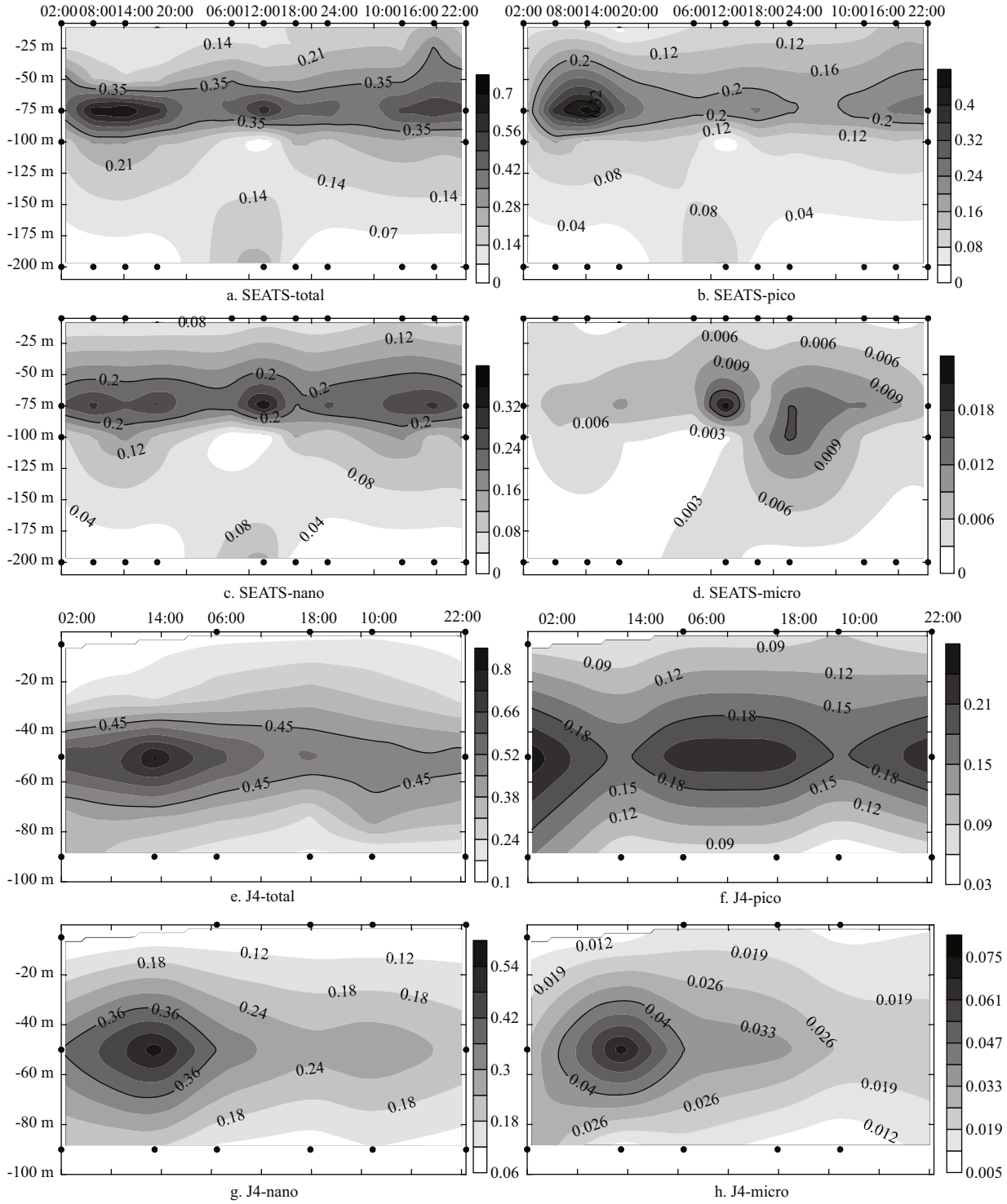

Fig.9 Temporal distribution of Chl *a* (μg/L) at mooring stations (SEATS & J4)

a–d. total, pico-, nano- and micro-class at station SEATS; e–h. total, pico-, nano- and micro- class at station J4.

station J4 were both found at 14:00, with an opposite pattern observed in the pico-size fraction. A high value of pico-size Chl *a* was found at 02:00, when the light level was low.

The reduced contribution of picoplankton Chl *a* to the total Chl *a* biomass at station J4 was owing to its relatively high nutrient concentrations, compared with offshore station SEATS (Agawin et al., 2000).

3.4 Effect of environmental factors on Chl *a*

Temperature, salinity and nutrient availability may play key roles in regulating spatial-temporal shifts

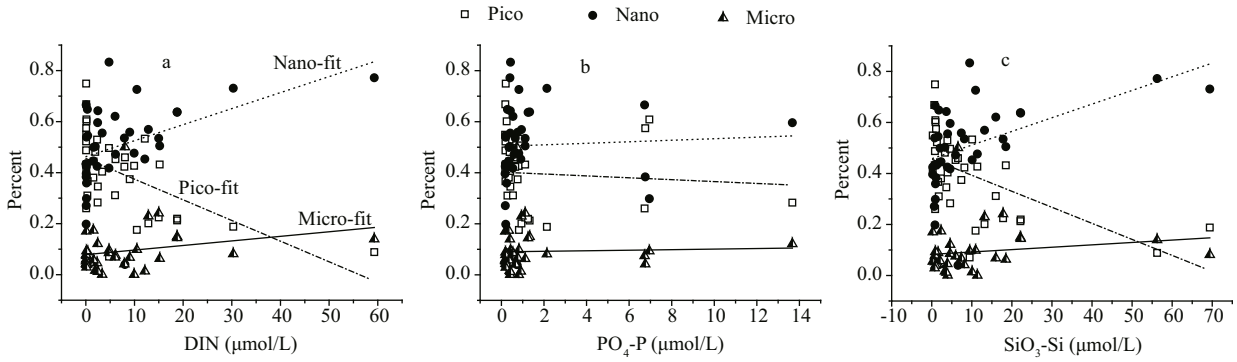

Fig.10 Relationships between fractionated chlorophyll *a* percent and nutrient mapping data at all water depths

Dissolved inorganic nitrogen is abbreviated as DIN, and included nitrate and nitrite.

between different sized fractions of Chl *a* biomass in the Zhujiang River estuary. However, the effects of individual environmental factors cannot be statistically separated (Agawin et al., 2000; Qiu et al., 2010).

Nutrient distribution in the surface layer at all stations is shown in Fig.6c. Relatively low concentrations were observed at the oceanic stations. However, patterns in the depth-weighted value of nutrient concentrations differed (Fig.6d), with less differences observed between coastal and offshore stations. Relationships between synchronized nutrient mapping data and fractionated Chl *a* compositions are shown in Fig.10. Significant negative correlations were observed between pico- Chl *a* and DIN (correlation coefficient, R^2=0.33) and SiO_3-Si (R^2=0.22). Both micro- and nano-Chl *a* were positively correlated with DIN (micro, R^2=0.05; nano R^2=0.2) and SiO_3-Si (micro, R^2=0.02; nano R^2=0.24). Phosphorus (P) values made no clear impact on all size fractions of Chl *a* (R^2=0.001–0.005), as P limitation was more locally (Sohm and Capone, 2006). Phosphorus in the ocean primarily comes from river runoff (Baturin, 2003), and thus phosphate concentration is likely to be limited in oligotrophic tropical waters. Comparative studies on the inner shelf and offshore area have shown that picoplankton has the opportunity to outgrow other size fractions in areas of high salinity and transmittance, with an affinity for low nutrient concentrations (Wawrik et al., 2003; Wang et al., 2014).

It is suggested that seawater delivered from the South China Sea water with high temperature and high salinity in the Luzon Strait and Kuroshio water has profound effects on the adjacent offshore realm, leading to low phytoplankton abundance (Tan et al., 2013). However, in the present study, the relatively large influence of the Zhujiang River plume mainly affects the structure and abundance of Chl *a* fractions in near shore stations. Thus, these two contrasting regions may be characterized by different biogeographic features.

Based on the distribution of phaeopigment in Fig.8e, we observed that phaeopigment concentrations tended to decrease offshore, with the exception of a lesser maxima at station SEATS. The vertical profile of phaeopigment was in parallel to total Chl *a*. The ratio of Phaeo to Chl *a* (Fig.8f) was highest at the 75 m water depth at station J5, suggesting phytoplankton death and settlement were more active here. Apart from the coastal stations influenced by the Zhujiang River discharge, phaeopigment contributes more to total Chl *a* at greater depths. It can be speculated that the conversion between phaeopigment and Chl *a* in the investigated region is mainly affected by light intensity and nutrient conditions. This might also imply higher grazing rates by zooplankton at these depths.

4 CONCLUSION

This study presents some important information to help understand the distribution and diurnal dynamics of the total and size-fractionated Chl *a* biomass in the NSCS. The mean total Chl *a* and phaeopigment concentrations in the investigated areas were 0.259±0.247 and 0.127±0.164 μg/L, respectively. The comparative study in coastal and offshore areas revealed apparent heterogeneity. Vertically, the maximum value appeared at depths of 30–50 m, and statistical analysis suggested significant vertical variations in Chl *a* biomass. In the study area, picoplankton and nanoplankton were the major components of the total Chl *a* biomass. The size-fractionated Chl *a* exhibited linear correlations with

nutrient concentrations. In addition, differential diurnal dynamics of total Chl *a* biomass and different Chl *a* size classes were observed in the two contrasting environments (coastal and oceanic area), which has not been reported in previously studies. The information presented here helps us better understand the spatial and temporal patterns in size-fractionated Chl *a* biomass in different regions of the NSCS and their major environmental controlling factors. This study will also contribute to our understanding of phytoplankton community structure and the environmental factors regulating the distribution of different phytoplankton functional groups in the NSCS.

5 ACKNOWLEDGEMENT

The authors would like to thank WEI Yuqiu, LI Zhuo and SHU Yi, as well as the captain and crew of R/V *Shiyanyi* for their assistance during the summer cruise. We thank Dr. CHEN Songze and his workmate from Tongji University for field nutrient seawater sampling. The synchronized nutrient data, provided by Dr. SUN Jia from Xiamen University, was also appreciated. Comments and suggestions from the editor, Professor Doug Campbell and two anonymous reviewers strengthened the manuscript.

References

Agawin N S R, Duarte C M, Agustí S. 2000. Nutrient and temperature control of the contribution of picoplankton to phytoplankton biomass and production. *Limnol*. *Oceanogr*., **45**(3): 591-600.

Azov Y. 1991. Eastern Mediterranean-a marine desert? *Mar*. *Poll*. *Bull*., **23**: 225-232.

Baturin G N. 2003. Phosphorus cycle in the ocean. *Lithol*. *Miner*. *Resour*., **38**(2): 101-119.

Berman T, Azov Y, Schneller A, Walline P, Townsend D W. 1986. Extent, transparency and phytoplankton distribution of the neritic waters overlying the Israeli coastal shelf. *Oceanol*. *Acta*, **9**(4): 439-447.

Bianchi T S, Findlay S, Fontvieille D. 1991. Experimental degradation of plant materials in Hudson river sediments. *Biogeochemistry*, **12**(3): 171-187.

Che H, Ran X B, Zang J Y, Liu J, Zheng L, Qiao F L, Zhan R. 2012. Distributions of size-fractions of Chlorophyll *a* and its controlling factors in summer in the southern South China Sea. *J*. *Hydroecol*., **33**(4): 63-72. (in Chinese with English abstract)

Chen C C, Kwo S F, Chung S W, Liu K K. 2006. Winter phytoplankton blooms in the shallow mixed layer of the South China Sea enhanced by upwelling. *J*. *Mar*. *Syst*., **59**(1-2): 97-110.

Fundel B, Stich H B, Schmid H, Maier G. 1998. Can phaeopigments be used as markers for *Daphnia* grazing in Lake Constance? *J*. *Plankton Res*., **20**(8): 1 449-1 462.

Gieskes W W C, Kraay G W, Baars M A. 1979. Current ^{14}C methods for measuring primary production: gross underestimates in oceanic waters. *Neth*. *J*. *Sea Res*., **13**(1): 58-78.

Goering J J, Dugdale R C, Menzel D W. 1964. Cyclic diurnal variations in the uptake of ammonia and nitrate by photosynthetic organisms in the Sargasso Sea. *Limnol*. *Oceanogr*., **9**(3): 448-451.

Gong G C, Liu K K, Liu C T, Pai S C. 1992. The chemical hydrography of the South China Sea west of Luzon and a comparison with the West Philippine Sea. *Terrestrial*. *Atmos*. *Ocean Sci*., **3**(4): 587-602. (in Chinese with English abstract)

Guo Y J, Ye J S, Zhou H Q. 1978. Quantitative distribution of phytoplankton in Xisha & Zhongsha Islands. *In*: Marine Biological Survey Research Reports in Xisha & Zhongsha Islands. Science Press, Beijing, China. p.1-10. (in Chinese)

Helling G R, Baars M A. 1985. Changes of the concentrations of chlorophyll and phaeopigment in grazing experiments. *Hydrobiol*. *Bull*., **19**(1): 41-48.

Ho A Y T, Xu J, Yin K D, Jiang Y L, Yuan X C, He L, Anderson D M, Lee J H W, Harrison P J. 2010. Phytoplankton biomass and production in subtropical Hong Kong waters: influence of the Pearl River outflow. *Estuar*. *Coast*, **33**(1): 170-181.

Hu Z F, Tan Y H, Song X Y, Zhou L B, Lian X P, Huang L M, He Y H. 2014. Influence of mesoscale eddies on primary production in the South China Sea during spring inter-monsoon period. *Acta Oceanol*. *Sin*., **33**(3): 118-128.

Iriarte A, Purdie D A. 1994. Distribution of chroococcoid cyanobacteria and size fractionated chlorophyll *a* biomass in the central and southern North Sea waters during June/July 1989. *Neth*. *J*. *Sea Res*., **31**(1): 53-56.

Jeffrey S W. 1980. Algal pigment systems. *In*: Falkowski P G ed. Primary Productivity in the Sea. Plenum Press, New York. p.35-38.

Jiao N Z, Ni I H. 1997. Spatial variations of size-fractionated chlorophyll, cyanobacteria and heterotrophic bacteria in the Central and Western Pacific. *Hydrobiologia*, **352**(1-3): 219-230.

Le F F, Ning X R. 2006. Variations of the phytoplankton biomass in the northern South China Sea. *J*. *Mar*. *Sci*., **24**(2): 60-69. (in Chinese with English abstract)

Le F F, Ning X R, Liu C G, Hao Q, Cai Y M. 2008. Standing stock and production of phytoplankton in the northern South China Sea during winter of 2006. *Acta Ecol*. *Sin*., **28**(11): 5 775-5 784. (in Chinese with English abstract)

Le F F, Sun J, Ning X R, Song S Q, Cai Y M, Liu C G. 2006. Phytoplankton in the northern South China Sea in summer 2004. *Oceanol*. *Limnol*. *Sin*., **37**(3): 238-248. (in Chinese with English abstract)

Li K Z, Guo Y J, Yin J Q, Huang L M. 2005. Phytoplankton diversity and abundance in Nansha islands waters in autumn of 1997. *J*. *Trop*. *Oceanogr*., **24**(3): 25-30. (in Chinese with English abstract)

Li T, Liu S, Huang L M, Zhang J L, Yin J Q, Sun L H. 2008.

Studies on a *Trichodesmium erythraeum* red tide in Daya Bay. *Mar*. *Environ*. *Sci*., **27**(3): 224-227. (in Chinese with English abstract)

Lin I I, Lien C C, Wu C R, Wong G T F, Huang C W, Chiang T L. 2010. Enhanced primary production in the oligotrophic South China Sea by eddy injection in spring. *Geophys*. *Res*. *Lett*., **37**(16): L16602.

Liu Z L, Ning X R, Cai Y M. 1998. Distribution characteristics of size-fractionated chlorophyll *a* and productivity of phytoplankton in the Beibu Gulf. *Acta Oceanol*. *Sin*., **20**(1): 50-57. (in Chinese with English abstract)

Lorenzen C J, Welschmeyer N A, Copping A E. 1983. Particulate organic carbon flux in the subarctic Pacific. *Deep Sea Res*., **30**(6): 639-643.

Ma W, Sun J. 2014. Characteristics of phytoplankton community in the northern South China Sea in summer and winter. *Acta Ecol*. *Sin*., **34**(3): 621-632. (in Chinese with English abstract)

Ning X, Chai F, Xue H, Cai Y, Liu C, Shi J. 2004. Physical-biological oceanographic coupling influencing phytoplankton and primary production in the South China Sea. *J*. *Geophys*. *Res*., **109**(C10): C10005.

Odate T, Maita Y. 1989. Regional variation in the size composition of phytoplankton communities in the western North Pacific ocean, spring 1985. *Biol*. *Oceanogr*., **6**(1): 65-77.

Parsons T R, Maita Y, Lalli C M. 1984. A Manual of Chemical and Biological Methods for Seawater Analysis. Pergamin Press, Oxford. p.173.

Peng X, Ning X R, Sun J, Le F F. 2006. Responses of phytoplankton growth on nutrient enrichments in the northern South China Sea. *Acta Ecol. Sin*., **26**(12): 3 959-3 968. (in Chinese with English abstract)

Platt T, Subba Rao D V, Irwin B. 1983. Photosynthesis of picoplankton in the oligotrophic ocean. *Nature*, **301**(5902): 702-704.

Polat S, Aka A. 2007. Total and size fractionated phytoplankton biomass off Karatas, north-eastern Mediterranean coast of Turkey. *Journal Black Sea/Mediterranean Environment*, **13**: 191-202.

Qiu D J, Huang L M, Zhang J L, Lin S J. 2010. Phytoplankton dynamics in and near the highly eutrophic Pearl River Estuary, South China Sea. *Cont*. *Shelf Res*., **30**(2): 177-186.

Schlitzer R. 2010. Ocean data view. http://odv.awi.de2010.

Shen P P, Tan Y H, Huang L M, Zhang J L, Yin J Q. 2010. Occurrence of brackish water phytoplankton species at a closed coral reef in Nansha Islands, South China Sea. *Mar*. *Pollut*. *Bull*., **60**(10): 1 718-1 725.

Shimada B M. 1958. Diurnal fluctuation in photosynthetic rate and chlorophyll *a* content of phytoplankton from Eastern Pacific Waters. *Limnol*. *Oceanogr*., **3**(3): 336-339.

Sohm J A, Capone D G. 2006. Phosphorus dynamics of the tropical and subtropical north Atlantic: *Trichodesmium* spp. versus bulk plankton. *Mar*. *Ecol*. *Prog*. *Ser*., **317**: 21-28.

Song X Y, Huang L M, Qian S B, Yin J Q. 2002. Phytoplankton diversity in waters around Nansha Islands in spring and summer. *Biodivers*. *Sci*., **10**(3): 258-268. (in Chinese with English abstract)

Su J L. 2005. Overview of the South China Sea circulation and its dynamics. *Acta Oceanol*. *Sin*., **27**(6): 1-8. (in Chinese with English abstract)

Sun J, Song S Q, Le F F, Wang D, Dai M H, Ning X R. 2007. Phytoplankton in the northern South China Sea in winter of 2004. *Acta Oceanol*. *Sin*., **29**(5): 132-145. (in Chinese with English abstract)

Suzuki R, Fujita Y. 1986. Chlorophyll decomposition in *Skeletonema costatum*: a problem in chlorophyll determination of water samples. *Mar*. *Ecol*. *Prog*. *Ser*., **28**: 81-85.

Tan J Y, Huang L M, Tan Y H, Lian X P, Hu Z F. 2013. The influences of water-mass on phytoplankton community structure in the Luzon strait. *Acta Oceanol*. *Sin*., **35**(6): 178-189. (in Chinese with English abstract)

Tang S M, Chen X Q. 2006. Phytoplankton diel rhythm in the waters of Quanzhou Bay in Fujian, China. *Acta Oceanol*. *Sin*., **28**(4): 129-137. (in Chinese with English abstract)

Wang B L, Liu C Q, Wang F S, Li S L, Patra S. 2014. Distributions of picophytoplankton and phytoplankton pigments along a salinity gradient in the Changjiang River Estuary, China. *J*. *Ocean Univ*. *China*, **13**(4): 621-627.

Wang Z H, Qi Y Z, Chen J F, Xu N, Yang Y F. 2006. Phytoplankton abundance, community structure and nutrients in cultural areas of Daya Bay, South China Sea. *J*. *Mar*. *Syst*., **62**(1-2): 85-94.

Wang Z H, Zhao J G, Zhang Y J, Cao Y. 2009. Phytoplankton community structure and environmental parameters in aquaculture areas of Daya Bay, South China Sea. *J*. *Environ*. *Sci*., **21**(9): 1 268-1 275.

Wawrik B, Paul J H, Campbell L, Griffin D, Houchin L, Fuentes-Ortega A, Muller-Karger F. 2003. Vertical structure of the phytoplankton community associated with a coastal plume in the Gulf of Mexico. *Mar*. *Ecol*. *Prog*. *Ser*., **251**: 87-101.

Ye J S, Lin Y S, Yuan W B. 1983. Quantitative distribution of phytoplankton in the East Sand Island sea area in summer. *In*: South China Sea marine biological research papers(I). Ocean Press, Beijing, China. p.1-6. (in Chinese)

Yentsch C S, Ryther J H. 2003. Short-term variations in phytoplankton chlorophyll and their significance. *Limnol*. *Oceanogr*., **2**(2): 140-142.

Zhang T H, Zhan H G, Chen C Q. 2007. Analyses on spatial variation of chlorophyll in surface layer of South China Sea. *J*. *Trop*. *Oceanogr*., **26**(5): 9-14.

Zhao H, Qi Y Q, Wang D X, Wang W Z. 2005. Study on the features of chlorophyll-*a* derived from SeaWifs in the South China Sea. *Acta Oceanol*. *Sin*., **27**(4): 45-52. (in Chinese with English abstract)

Zhao J, Yao P, Yu Z G. 2010. Progress in marine sedimentary pigments as biomarkers. *Advances in Earth Science*, **25**(9): 950-959. (in Chinese with English abstract)

Zhou W H, Yuan X C, Huo W Y, Yin K D. 2004. Distribution of chlorophyll a and primary productivity in the adjacent sea area of Changjiang River Estuary. *Acta Oceanol*. *Sin*., **26**(3): 143-150. (in Chinese with English abstract)